

Final Technical Report Submitted to the

**U. S. Department of Energy**

**Office of Energy Research**

By: Purdue Research Foundation  
West Lafayette, IN 47907

Title: **Multiresonant Spectroscopy and the High-Resolution  
Threshold Photoionization of Combustion Free Radicals**

Research Ending: August 1, 2003

Principal Investigator: Edward R. Grant  
Department of Chemistry

## **Abstract**

This report describes the results of a program of research on the thermochemistry, spectroscopy and intramolecular relaxation dynamics of the combustion intermediate, HCO. We prepare this radical from acetaldehyde as a photo-precursor in a differentially pumped laser-ionization source quadrupole mass spectrometer. Using a multiresonant spectroscopic technique established in our laboratory, we select individual rotational states and overcome Franck-Condon barriers associated with neutral-to-cation geometry changes to promote transitions to individual autoionizing series and state-resolved ionization thresholds. Systematic analysis of rotational structure and associated lineshapes provide experimental insight on autoionization dynamics as input for theoretical modeling. Extrapolation of series, combined with direct threshold-photoelectron detection, yield precise ionization potentials that constitute an important contribution to the thermochemical base of information on HCO.

## Introduction

Research in this DOE-sponsored program has used laser spectroscopy to gather experimental information about the molecular structure, thermochemistry and intramolecular dynamics of combustion free radicals and the cations they form. Our specific objectives have been:

- To measure ionization potentials with wavenumber accuracy for polyatomic free radicals of importance to combustion.
- To characterize the vibrational structure of the corresponding closed-shell cations derived from these free radicals, including a determination of anharmonic coupling and intramolecular vibrational relaxation in higher vibrationally excited states.
- To gather information from electronic transitions that provides spectroscopic constants for neutral radical ground states that can be useful for diagnostic development.
- To determine rotationally detailed state-to-state photoionization cross sections for comparison with theory.
- By frequency-domain analysis of rotationally resolved high-Rydberg spectra, to study near ionization threshold electron-cation scattering dynamics that are relevant, for example, to plasma processes such as dissociative recombination.

Efforts in the period of this contract progressed well in each of the above areas. In work on the formyl radical, we extended a method introduced sometime ago for NO to greatly improve the signal-to-noise ratio in the ionization-detected ultraviolet absorption spectra of HCO and DCO.<sup>1</sup> In this approach, which we term assisted-REMPI, an additional high-power visible laser field drives the photoionization of levels populated by lower-power discrete-discrete transitions.<sup>2</sup> We used this technique to uncover a number of new features in the  $3p\pi^2\Pi \leftarrow X^2A'$  systems of HCO and DCO. From these data, we produced a comprehensive assignment of levels split by Renner-Teller coupling, including an assessment of (04<sup>0</sup>0)-(100) Fermi resonance in the DCO<sup>+</sup> core.

We recorded high-Rydberg series of HCO converging to individual rotational levels of the (03<sup>1</sup>0) and (03<sup>3</sup>0) states of the cation.<sup>3</sup> Extrapolation of this structure provides information on the energy positions of these vibrational levels and refines our earlier estimates of the anharmonicity of bending for comparison with high-level *ab initio* calculations. Positions computed for higher excited states agree quite well with measurements for HCO.

A program of experiments on DCO progressed to provide us with a similar level of understanding on the rovibrational structure of the deuterated cation. Devising an

approach that we call double-resonant photoionization efficiency (DR/PIE) spectroscopy,<sup>4</sup> we have established the ionization potential of DCO to within 3 cm<sup>-1</sup>. This limit together with that for the formation of the lowest rotational level of the (010) state of DCO<sup>+</sup>, established by Rydberg extrapolation, provided the first precise determination of the fundamental bending frequency of the deuterated formyl cation.

Further experiments on DCO extended Rydberg-Rydberg double resonance measurements to series that converge to ion levels associated with the first, second and third overtones of the bend.<sup>5,6</sup> These results establish precise rovibrational positions for comparison with theory. We found that available calculations fit well with the positions that we have measured at lower vibrational energies. Comparisons for higher energy levels show that theory underestimates the anharmonicity of bending and fails to predict a significant Fermi resonance that couples the (04<sup>0</sup>) state with the CD-stretch fundamental.

We photolyzed diborane to produce BH. In scans over the region from 369 to 372 nm, we obtained the one-photon spectrum of the A <sup>1</sup>Π (v' = 2) ← X <sup>1</sup>Σ<sup>+</sup> (v'' = 0) transition in (1+2)-photon ionization-detected absorption.<sup>7</sup> The two-photon ionization step is enhanced by an adventitious near-resonance with the v = 1 level of the B <sup>1</sup>Σ<sup>+</sup> state at the energy of the second photon. Further experiments exploited the large cross sections for absorption sequences such as this to record two- and three-color multi-resonant spectra of the high-Rydberg states of this important CVD transient.

In an effort to establish first-photon transitions for three-color triple-resonance experiments on formyl radical, we obtained ion-dip spectra of transitions in the A <sup>2</sup>A'' ← X <sup>2</sup>A' system of HCO.<sup>8</sup> Fixing an ionization laser on a single rotational feature in the ultraviolet 3pπ <sup>2</sup>Π (030) ← X <sup>2</sup>A' (000) band, we recorded depletion signals that appeared when we scanned a second visible laser through allowed transitions in the A ← X system. Positions provide spectroscopic information on the A <sup>2</sup>A'' state. Linewidths reflect the rates of radiationless relaxation to the continuum of the X <sup>2</sup>A' state.

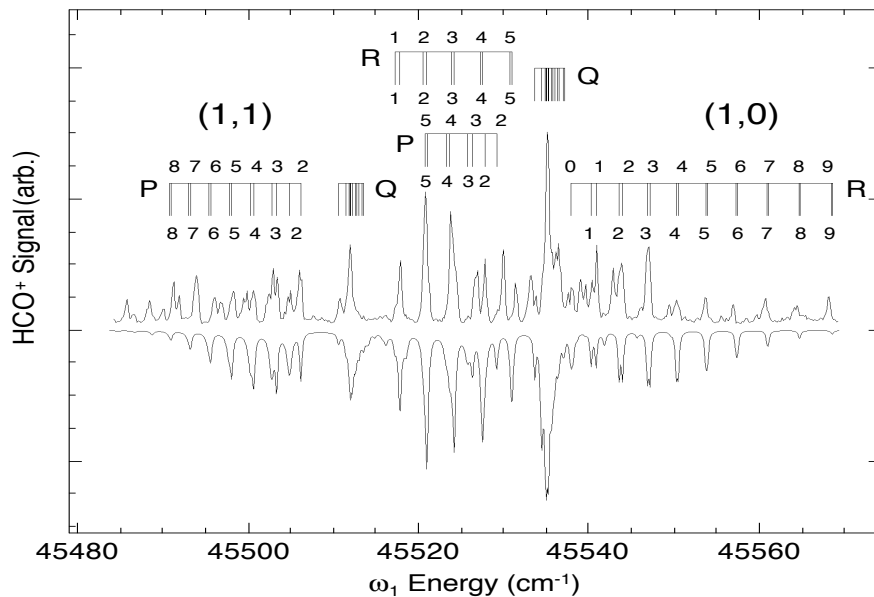
We succeeded in obtaining the first REMPI spectrum of the vinoxy radical.<sup>9</sup> One-color scans over the range from 345 to 328 nm yielded a progression of vibrational bands, which parallels a system that appears at similar energy in the isoelectronic molecule, NO<sub>2</sub>.

# Summary of Recent Progress in DOE Sponsored Research

## *Laser-assisted (1+1')-photon resonant ionization-detected absorption spectroscopy of the $3p\pi^2\Pi$ state of HCO and DCO*

Work in our laboratory to characterize the thermochemistry of the HCO radical and the rovibrational structure of  $\text{HCO}^+$  relies on the selectivity of vertical Rydberg-Rydberg transitions in the radical.<sup>10-14</sup> Success requires secure assignment of ultraviolet first-photon transitions to the  $3p\pi^2\Pi$  intermediate state. We found in contract research that a second, high-power visible laser, used as an ionization field, significantly enhances the sensitivity of ionization-detected absorption as a means to locate transition energies in the  $3p\pi^2\Pi \leftarrow X^2A'$  systems of HCO and DCO.<sup>2</sup> For example, it is only with difficulty that conventional ultraviolet (1+1)-photon ionization spectroscopy resolves the Franck-Condon unfavorable  $3p\pi^2\Pi(000) \leftarrow X^2A'(000)$  origin for HCO. This transition is not seen at all for DCO. Using a visible laser to drive the ionization step, origin band systems emerge clearly for both systems, as shown below in Figure 1.

We recorded (1+1')-photon resonant-ionization spectra of higher vibrationally excited states in the  $3p\pi^2\Pi$  systems of HCO and DCO. Visible laser assistance revealed numerous transitions to higher vibronic angular momentum components in Renner-Teller split bending progressions. Analysis of this structure enabled an unambiguous assignment of the (001) fundamental and a clear measure of the effect of (040) – (100) bend-stretch Fermi resonance on Renner-Teller coupling in this state.



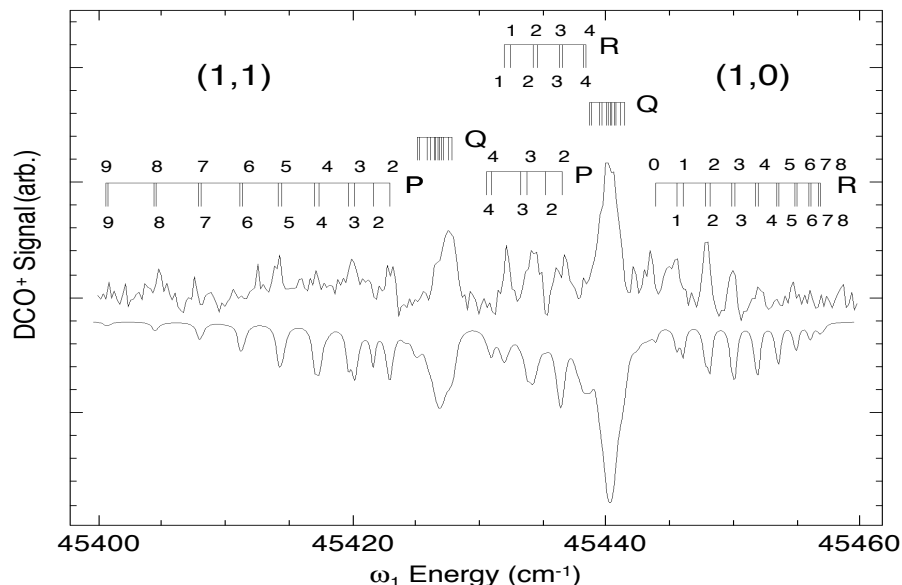


Figure 1. Laser-assisted (1+1')-photon ionization-detected absorption spectra of the (000) band of the  $3p\pi$   $^2\Pi$  Rydberg state in HCO (top) and DCO (bottom) with simulations (inverted). Parenthetical quantum numbers are (K',K''), referring to the principal axis projections of the excited and ground-state total angular momentum.

### *Experimental Characterization of the Higher Vibrationally Excited States of HCO<sup>+</sup>: Determination of $\omega_2$ , $x_{22}$ , $g_{22}$ and $B_{[030]}$*

The rovibrational spectroscopy of HCO<sup>+</sup> has served as a benchmark in the experimental and theoretical understanding of molecular cationic structure. HCO<sup>+</sup> is the most important cation in hydrocarbon combustion.<sup>15-18</sup> It is the first polyatomic cation to be characterized by application of infrared and microwave absorption spectroscopies.<sup>19-28</sup> This system continues to serve as a prominent point of contact between experiment and *ab initio* theories of molecular electronic structure.<sup>29-33</sup> However, despite this fundamental importance and the great deal of experimental work that had been carried out on HCO<sup>+</sup> over the last 25 years, laboratory measurements had securely determined spectroscopic parameters only for the ground state and three fundamental vibrationally excited states of this system.

During the contract period, we acquired and analyzed spectra of high Rydberg series of HCO built on the (030) vibrational state of the core in order to establish rovibrational state-detailed thresholds for the (030) level of HCO<sup>+</sup>.<sup>3</sup> Strongly vertical Rydberg-Rydberg transitions from photoselected  $N' = 0$  and  $N' = 2$  rotational levels of the  $\Sigma^-$  Renner-Teller vibronic component of the  $3p\pi$   $^2\Pi$  (030) complex define individual series converging to rotational levels,  $N^+ = 1$  through 5, and 3 through 5 of the HCO<sup>+</sup> vibrational states (03<sup>1</sup>0) and (03<sup>3</sup>0), respectively. Figure 2 shows a portion of the spectrum observed from  $3p\pi$   $^2\Pi$  (030)  $\Sigma^-$   $N' = 0$ , together with a simulation. Prominent

resonances can be identified that have quantum defects closely related to ones identified in a comprehensive assignment of series converging to the (010) state of  $\text{HCO}^+$ .

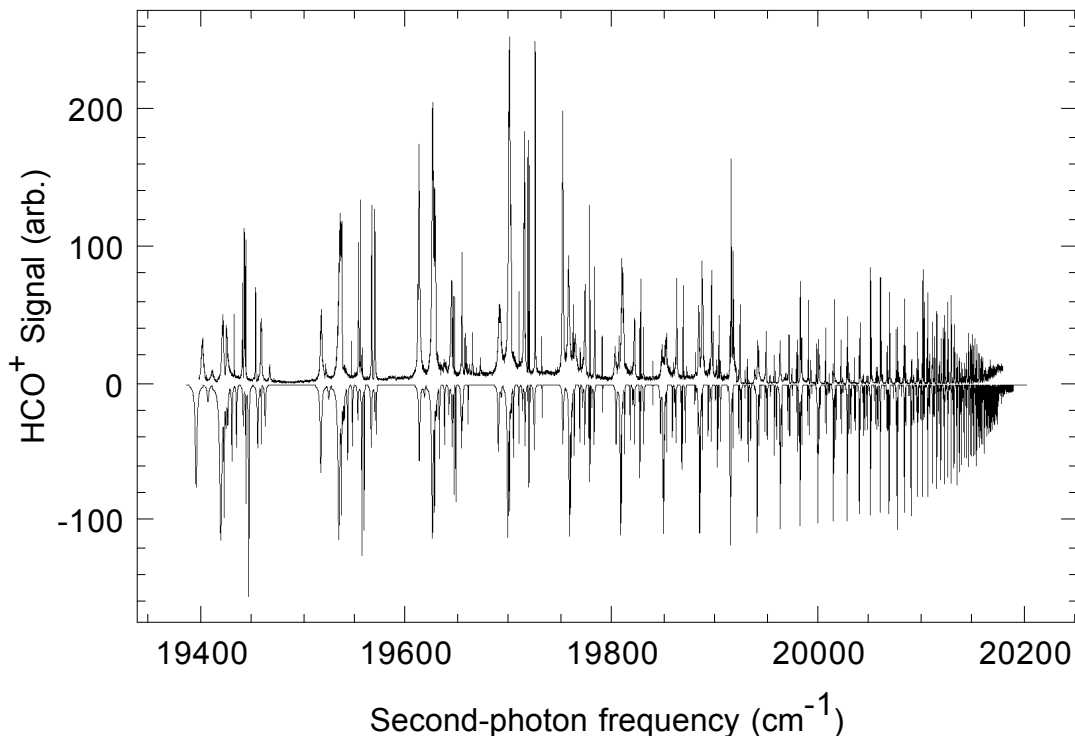


Figure 2. Spectrum of  $\text{HCO}^+$  autoionization resonances obtained in transitions from the  $N' = 0$  level of the  $\Sigma^-$  component of the  $3p\pi^2\Pi$  (030) system (upper trace). Simulation drawn from quantum defects established by analogy to our comprehensive assignment of Rydberg series built on the (010) state of  $\text{HCO}^+$ .

Extrapolation of autoionizing series in the (030) spectrum locates the positions of  $\text{HCO}^+$  rovibrational states associated with the second bending overtone to better than  $\pm 0.1 \text{ cm}^{-1}$ . The use of this information combined with precise ionization limits for lower vibrational states determined from earlier Rydberg extrapolations and spectroscopic information available from infrared absorption measurements enables us to accurately estimate the force-field parameters for  $\text{HCO}^+$  bending. Parameters derived from our measurements include the harmonic bending frequency,  $\omega_2$ , the vibrational angular momentum splitting constant,  $g_{22}$ , and the diagonal bending anharmonicity,  $x_{22}$ .

*Double-resonant photoionization efficiency (DR/PIE) spectroscopy: A precise determination of the adiabatic ionization potential of DCO*

While infrared data for the  $\nu_2$  fundamental combines well with our measurements on the higher excited states to produce a rather complete picture of bending in  $\text{HCO}^+$ , the base of knowledge available from conventional spectroscopy concerning the deuterated isotopomer is much less secure. Analogy with isoelectronic HCN suggests that  $\text{DCO}^+$

plays an important role in determining the isotopic composition of astrophysical polyatomics.<sup>35</sup> CD- and CO-stretch fundamentals have been observed by infrared absorption,<sup>35,36</sup> but until our work in the contract period, bending excited states had been observed only by their rotational structure in microwave spectra,<sup>37-40</sup> and the only available estimate of the ionization potential of DCO was an approximate value extrapolated from displaced progressions in the bent-to-linear photoelectron spectrum.<sup>41</sup>

Introducing a new technique, which we term double-resonance photoionization efficiency (DR/PIE) spectroscopy, we made the first high-resolution measurement of the adiabatic ionization potential of DCO and determined the fundamental bending frequency of DCO<sup>+</sup>.<sup>4</sup> Fixing a first-laser frequency on selected ultraviolet transitions to individual rotational levels in the (000) band of the  $3p\pi^2\Pi$  intermediate Rydberg state of DCO, we have scanned a second visible laser over the range from 20000 to 20300  $\text{cm}^{-1}$  to record DR/PIE spectra. Intermediate resonance with this Rydberg state facilitates transitions to the threshold for producing ground-state cations by bridging the Franck-Condon gap between the bent neutral radical and linear cation. Selecting a single rotational state for ionization, we used double-resonant excitation to eliminate thermal congestion. Spectroscopic features for first-photon resonance were identified by reference to a complete assignment of the  $3p\pi^2\Pi$  (000)  $\leftarrow X^2A'$  (000) band system of DCO. By calibration with HCO, for which the adiabatic ionization threshold is accurately known, we established an instrument function for this experiment that accounted for collisional effects on the shape of the photoionization efficiency spectrum near threshold. Analysis of the DR/PIE threshold for DCO yielded an adiabatic ionization threshold of  $65616 \pm 3 \text{ cm}^{-1}$ .

By extrapolation of vibrationally autoionizing Rydberg series reached in double-resonant transitions from the  $\Sigma^+$  component of the  $3p\pi^2\Pi$  (010) intermediate state, we determined an accurate rotationally state-resolved threshold for producing DCO<sup>+</sup> (010). This energy, together with the threshold determined for the vibrational ground state of the cation provided a first estimate of the bending frequency for DCO<sup>+</sup> as  $666 \pm 3 \text{ cm}^{-1}$ . Assignment of the (010) autoionization spectrum further yielded a measurement of an energy of  $4.83 \pm 0.01 \text{ cm}^{-1}$  for the (2-1) rotational transition in the  $^1\Sigma^+$  (01<sup>1</sup>0) state of DCO<sup>+</sup>. Figure 1 shows an ionization-detected absorption spectrum of Rydberg states built on the fundamental bending excited state of DCO<sup>+</sup>, selected in transitions from  $3p\pi^2\Pi$  (010)  $\Sigma^+ N' = 0$ . The simulation identifies resonances converging to rovibrational thresholds  $N^+ = 1, 2$  and  $3$  in  $^1\Sigma^+$  (010) DCO<sup>+</sup>.

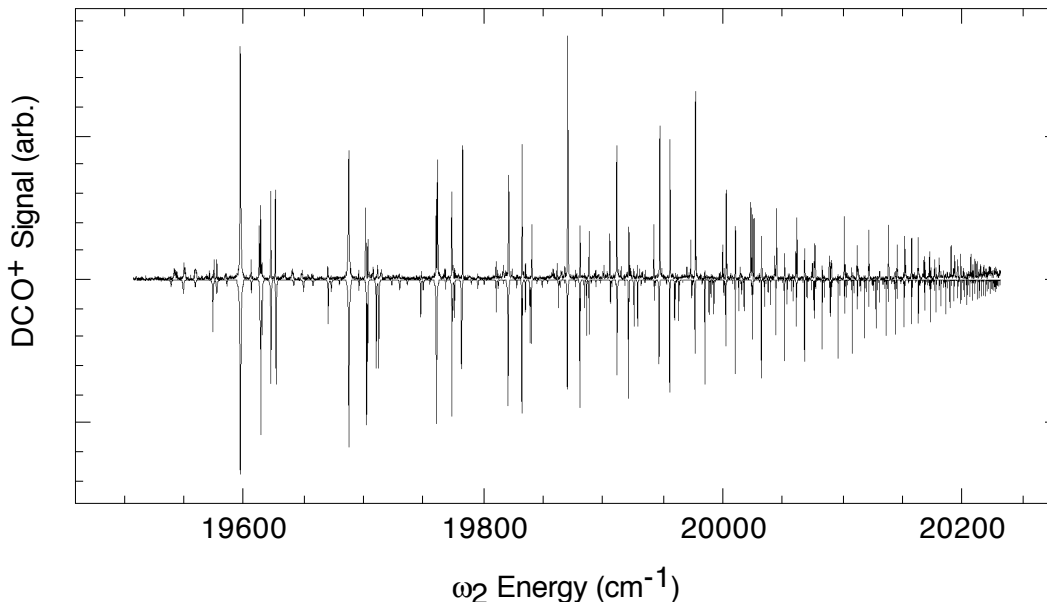


Figure 3. Scan of  $\omega_2$  from the adiabatic ionization threshold to the vertical limit for producing  $\text{DCO}^+$  (010) originating from the  $3p\pi^2\Pi(010)\Sigma^+N^l=0$  intermediate state. Inverted simulation based on Rydberg parameters for series of constant quantum defect converging to rotational levels  $N^+ = 1, 2$  and  $3$  in the (010) vibrational state of  $\text{DCO}^+$ .

### *An experimental measure of anharmonicity in the bending of $\text{DCO}^+$*

Extrapolating rovibrationally isolated Rydberg series of  $\text{DCO}$  to higher vibrationally excited states of  $\text{DCO}^+$ , we produced a map, with sub-wavenumber accuracy, of individual rotational level positions in the (02<sup>0</sup>0) and (02<sup>2</sup>0) states of  $\text{DCO}^+$ .<sup>5</sup> By analysis of this structure, we determined the rotational constant  $B_{[020]}$ , and measured the frequency of the bending overtone, from which we determined the spectroscopic parameters  $\chi_{22}$ ,  $g_{22}$ , and derived an estimate of the harmonic bending frequency,  $\omega_2$ . Rotational properties of excited  $\text{DCO}^+$  found by Rydberg extrapolation are observed to agree well with quantities measured by microwave spectroscopy. The CASSCF-MRCI potential energy surface of Puzzarini and coworkers,<sup>30</sup> which yields fundamental frequencies that agree with experiment for  $\text{HCO}^+$ , is shown to conform well with these first measurements of the bending frequencies of  $\text{DCO}^+$ .

### *Bend-Stretch Fermi Resonance in $\text{DCO}^+$*

Perturbations in the positions of higher vibrational states of polyatomic molecules confer information on the anharmonic properties of vibrational potentials that permit energy to flow between zeroth-order normal modes. Such details present a serious challenge to theory in efforts to predict rates from *ab initio* calculations. Before our work, there were no measurements on the positions of higher vibrationally excited states of either  $\text{HCO}^+$  or  $\text{DCO}^+$ , but conjectures on anharmonicity were possible based on rotational structure.

Microwave satellite transitions assigned to the  $2750\text{ cm}^{-1}$   $\nu_1$  C-D stretch excited state evidence an anomalously high rotational constant.<sup>36</sup> Hirota and coworkers have attributed this to a Fermi resonance between (100) and the totally symmetric component of (040) which can be estimated to fall in the same energy region.<sup>39</sup> *Ab initio* calculations, which return accurate estimates for all of the fundamental frequencies and first few overtones, show no evidence of such coupling,<sup>30-32</sup> and Botschwina and Sebald have suggested instead that (100) couples with (011) by means of a *l*-doubling interaction.<sup>42</sup>

From double-resonant Rydberg extrapolations that rotationally resolve limits associated with the bending-excited levels (030) and (040), we collected direct information on the structure of the bend.<sup>6</sup> We found that analysis of the rovibrational structure derived from the positions of the (030) thresholds agrees with a simple parameterization extended from a fit to lower vibrational levels. For (040), however, we found the vibrational angular momentum components (04<sup>0</sup>0) and (04<sup>2</sup>0) *inverted* in energy, with the (04<sup>0</sup>0) component displaced approximately  $20\text{ cm}^{-1}$  to a position above that of (04<sup>2</sup>0). We interpreted this perturbation to support Hirota's conjecture that the vibrational structure of DCO<sup>+</sup> is perturbed by a 4:1 bend-stretch Fermi resonance. Extending the pattern by which vibrational angular momentum components are split in (020) and (030), we established the unperturbed position of (04<sup>0</sup>0), from which we estimated the matrix element for bend-stretch coupling. Analysis yielded a moderate Fermi matrix element,  $W_{(04^0_0)(10^0_0)}$ , of  $32.43\text{ cm}^{-1}$ , which is about two-thirds the magnitude of coupling found in the systems, CO<sub>2</sub> and NO<sub>2</sub><sup>+</sup>, where bend-stretch mixing significantly affects the character of higher vibrationally excited states.<sup>43</sup>

### *Appearance of the $A^1\Pi \leftarrow X^1\Sigma^+$ transition in the (1+2)-photon ionization-detected absorption spectrum of BH*

We obtained the mass-selected resonance-enhanced multiphoton ionization (REMPI) spectrum of diatomic boron hydride.<sup>7</sup> BH fragments were formed by the 193 nm photolysis of B<sub>2</sub>H<sub>6</sub> entrained in H<sub>2</sub> in a pulsed free-jet expansion. Over the spectral range from 368 to 372 nm, we found rotational line features at time-of-flight resolved cation masses  $m = 12$  (<sup>11</sup>BH<sup>+</sup>),  $m = 11$  (<sup>10</sup>BH<sup>+</sup>, <sup>11</sup>B<sup>+</sup>) and  $m = 10$  (<sup>10</sup>B<sup>+</sup>). Figure 1 shows an example for mass  $m = 12$ . All lines observed in this spectrum and the ones recorded for lighter masses can be assigned to the one-photon transition,  $A^1\Pi(v' = 2) \leftarrow X^1\Sigma^+(v'' = 0)$ , in <sup>11</sup>BH or its less-abundant isotopomer, <sup>10</sup>BH. Cation production at these wavelengths requires three photons. This signal must therefore reflect resonant one-photon absorption followed by two-photon ionization in a (1+2)-photon process. This work represents the first observation of the well-characterized  $A^1\Pi \leftarrow X^1\Sigma^+$  system in ionization spectroscopy and the first measurement of line positions in the  $A^1\Pi v = 2$  state for <sup>10</sup>BH.

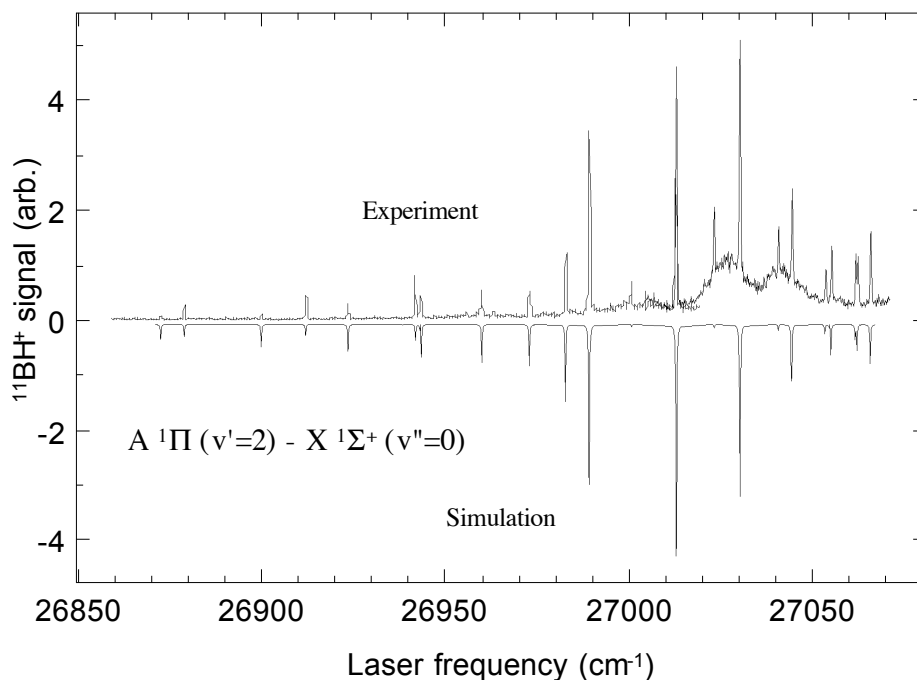


Figure 4. Mass-resolved (1+2)-photon ionization-detected absorption spectrum of  $^{11}\text{BH}^+$  (upper trace). Simulation of the one-photon  $\text{A } ^1\Pi (v'=2) - \text{X } ^1\Sigma^+ (v''=0)$  transition for a bimodal rotational state distribution characterized by temperatures of 40 K (0.9) and 600 K (0.1) (lower trace).

$^{11}\text{BH}$  spectroscopic parameters established by Fernando and Bernath<sup>44</sup> from an analysis of the (0,0), (1,1) and (2,2) sequence bands, extended well to describe the (2,0) transition we observed for  $^{11}\text{BH}$ . Adjusting the constants for mass we found good correspondence for  $^{10}\text{BH}$  bands as well, though slightly larger residual errors raise the question of non-adiabatic contributions.

Examination of the energy spacing of electronically excited states in BH showed that this (1+2)-photon ionization pathway is likely assisted by a near-resonance with the  $v = 1$  level of the  $\text{B } ^1\Sigma^+$  state at the energy of the second photon. The efficiency of this ionization route suggests that the  $\text{A } ^1\Pi$  excited state will serve as an effective gateway in two- and three-color strategies to probe the structure and dynamics of the higher excited states of this reactive intermediate.

### *Ion-dip absorption spectroscopy of the $\text{A } ^2\text{A}''$ State of $\text{HCO}$*

We initiated experiments to establish  $^2\text{A}''$  levels suitable for double resonance in two-color transitions to higher vibrational levels of the  $3p\pi$  Rydberg state. Promising candidates have been observed in laser-induced fluorescence.<sup>47</sup> This system has been well studied by a variety of other spectroscopic techniques, including four-wave mixing<sup>48</sup> and photofragment excitation,<sup>49</sup> as well as optogalvanic spectroscopy.<sup>50</sup> All levels accessed in visible absorption predissociate with lifetimes varying from tens of picoseconds to hundreds of femtoseconds.

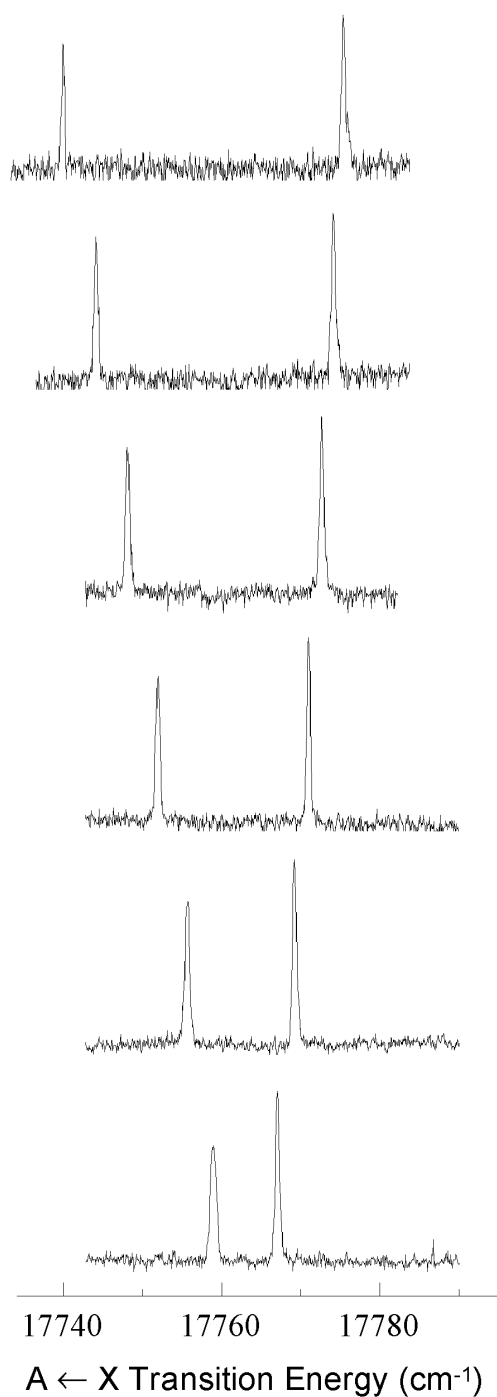


Figure 5 Ion dip spectra of the  $A \leftarrow X$  transition in HCO for a series of selected initial rotational states from  $N'' = 1-6$

To identify  $A \ ^2A'' \leftarrow X \ ^2A'$  transitions in our apparatus, we performed ion-dip experiments. Tuning an ionization laser to transitions in the  $3p\pi \ ^2\Pi (030) \leftarrow X \ ^2A'$  system, we dipped the ion signal by pumping transitions from the selected  $X \ ^2A'$  level to the  $A \ ^2A''$  state. Figure 5 to the right shows a sequence of scans over  $A \ ^2A'' (0 \ 11^0 \ 0) \leftarrow X \ ^2A' (000)$  for  $3p\pi \ ^2\Pi (030) \leftarrow X \ ^2A'$  resonant ionization transitions fixed on initial rotational quantum numbers  $N''$  from 0 to 9. These lines associated with an odd bending level of the  $^2A''$  state appear comparatively sharp because predissociation to the underlying  $A'$  continuum requires indirect K-type and Coriolis coupling. Lifetimes determined by high-resolution observations lie in the range of tens of picoseconds.<sup>50</sup> By comparison, Figure 6 below shows a spectrum of the  $A \ ^2A'' (0 \ 10^1 \ 0) \leftarrow X \ ^2A' (000)$  band recorded from the  $N''=1$  level of the ground state. The simulations represent Lorentzians reflecting lifetimes of 150 fs.

Double resonance with the  $A \ ^2A'' (0 \ 11 \ 0)$  state offers a feasible means to populate higher bending excited levels of the  $3p\pi \ ^2\Pi$  state. From the measured lifetime, we can estimate that temporally overlapped 5 ns lasers will effect population transfers within a factor of 100 as large as those that could be achieved by one-photon excitation. Favorable Franck-Condon factors could well improve the effectiveness of this spectroscopic route, as will the reduction in non-resonant background that can be expected using longer wavelength light sources. In practice, however, our preliminary experiments have shown that required second photon frequencies produce background signal from ionization of our acetaldehyde precursor. The use of  $H_2CO$  should yield no such contaminating signal. Sections below discuss a means for efficiently generating HCO radicals from this source.

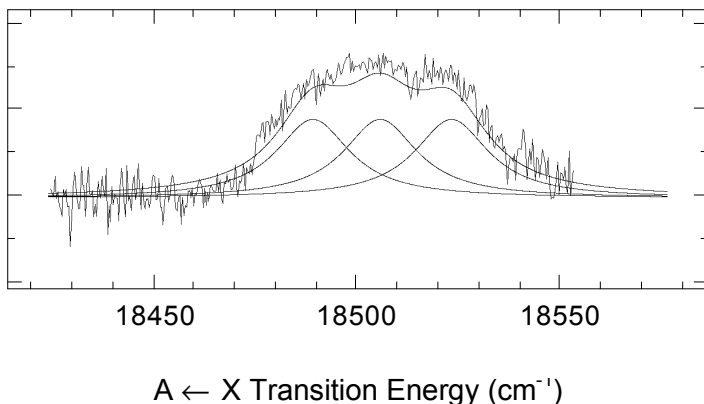


Figure 6 Ion dip spectra of the A  $^2A''$  (0 12 0)  $\leftarrow$  X  $^2A'$  transition in HCO for an initial rotational states,  $N'' = 6$ . Simulations use (0 11 0) rotational constants with Lorentzian widths corresponding to lifetimes of 150 fs.

### *Ionization-detected two-photon absorption spectrum of vinoxy radical*

The vinoxy radical is important in combustion as an intermediate in the oxidation of terminal alkenes.<sup>51</sup> It is readily formed in the 193 nm photolysis of alkyl vinyl ethers.<sup>52</sup> Considerable spectroscopic work on this system has thoroughly characterized the ground state and the brightly fluorescent B  $^2A''$  state.<sup>53-58</sup> This data provides the information necessary to benchmark *ab initio* calculations and develop diagnostics in order to probe the reaction dynamics of this radical.

Just as HCO can to a certain extent be viewed as a pseudo-diatomic, isoelectronic with NO, the molecular orbitals filled to assemble the CH<sub>2</sub>-CH-O backbone of vinoxy map on those of the 17-electron triatomic, NO<sub>2</sub>. Like NO<sub>2</sub>, vinoxy forms a closed shell cation. This feature of NO<sub>2</sub> confers stability on its Rydberg states, enabling a precise measure of its state-to-state ionization energies, as well as a comprehensive characterization of the rovibrational structure of the cation core and the dynamics of its interaction with extravalent electrons.<sup>45,59,60</sup> By analogy, we expected it to be possible to gain similar information on the higher excited neutral and cationic states of vinoxy radical. However, despite the importance of this thermochemical information, and the interesting additional structural and dynamic dimensions afforded by CH<sub>x</sub> vibrational modes, there have been no reported efforts to obtain an ionization spectrum of vinoxy, multiresonant or otherwise.

In contract experiments, we succeeded in recording a single-color ionization-detected two-photon absorption spectrum of vinoxy radical.<sup>9</sup> The structure we observed consisted of vibrational progressions that resemble those found at a very similar energy in the (2+1)-photon ionization spectrum of the 3ps  $^2\Sigma_u^+$  Rydberg state of NO<sub>2</sub>.<sup>61</sup> By means of *ab initio* calculations, we estimated the ionization potential of vinoxy to lie close to that of NO<sub>2</sub>.<sup>62</sup> Thus, it seems reasonable to associate this structure with a similar 3p Rydberg orbital built on the CH<sub>2</sub>CHO core. A comparable system is observed in allyl radical,<sup>63</sup> which can also be viewed as isoelectronic, although with a much lower ionization potential.

Figure 7 shows a portion of this new ionization-detected absorption spectrum of vinoxy radical.

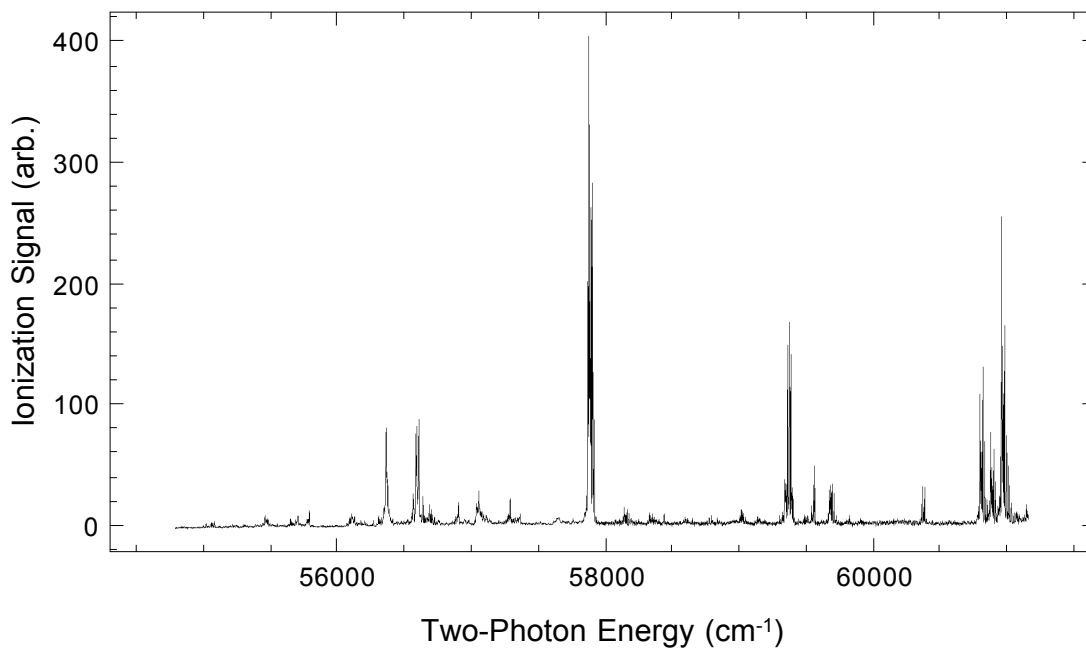


Figure 7 Ionization-detected two-photon absorption spectrum of vinoxy radical produced by the 193 nm photolysis of ethyl vinyl ether in a pulsed free-jet expansion.

## References

1. R. J. Foltynowicz, J. D. Robinson, K. Prentice, P. Bell and E. R. Grant, *J. Chem. Phys.* **116**, xxxx (2002).
2. E. Kolodney, P. S. Powers, L. Hodgson, H. Reisler and C. Wittig, *J. Chem. Phys.* **94**, 2330 (1991); M. Hippler and J. Pfab, *Chem. Phys. Lett.* **243**, 500 (1995); R. Uberna, R. D. Hinchliffe and J. I. Cline, *J. Chem. Phys.* **105**, 9847 (1996).
3. R. J. Foltynowicz, J. D. Robinson, E. J. Zückerman, H. G. Hedderich and E. R. Grant, *J. Mol. Spectrosc.* **199**, 147-157 (2000).
4. R. J. Foltynowicz, J. D. Robinson and E. R. Grant, *J. Chem. Phys.* **114**, 5224 (2001).
5. R. J. Foltynowicz, J. D. Robinson and E. R. Grant, *J. Chem. Phys.* **115**, 878 (2001).
6. J. D. Robinson, R. J. Foltynowicz, K. Prentice, P. Bell and E. R. Grant, *J. Chem. Phys.* **116**, 2370 (2002).
7. J. Clark, M. Konopka, L.-M. Zhang and E. R. Grant, *Chem. Phys. Lett.* **340**, 45 (2001).
8. J. D. Robinson, R. J. Foltynowicz, K. Prentice and E. R. Grant, to be published.
9. K. Prentice, R. Niccodeamus J. and E. R. Grant, to be published..
10. E. E. Mayer and E. R. Grant, *J. Chem. Phys.* **103**, 10513 (1995).
11. E. E. Mayer, H. G. Hedderich and E. R. Grant, *J. Chem. Phys.* **108**, 1886 (1998).
12. E. E. Mayer, H. G. Hedderich and E. R. Grant, *J. Chem. Phys.* **108**, 8429 (1998)
13. E. R. Grant, *On the high Rydberg states of the formyl radical and the dynamics of vibrational autoionization in triatomic molecules*, in, *The Role of Rydberg States in Spectroscopy and Reactivity*, C. Sandorfy, ed. (Kluwer Academic Publishers, Dordrecht, 1998).
14. J. D. Robinson, R. J. Foltynowicz and E. R. Grant, *J. Chem. Phys.* **112**, 1679-1684 (2000).
15. M. MacGregor and R. S. Berry, *J. Phys. B* **6**, 181 (1973).
16. N. Jonathan, A. Morris, M. Okuda and D. J. Smith, *J. Chem. Phys.* **55**, 3046 (1971).
17. A. Fontijn, *Pure Appl. Chem.* **39**, 287 (1974).

18. J. Warnatz, in *Combustion Chemistry*, W. C. Gardiner, Jr., ed. (Springer-Verlag, Berlin, 1984), p. 197.
19. R. C. Woods, T. A. Dixon, R. J. Saykally and P. G. Szanto, *Phys. Rev. Lett.* **35**, 1269 (1975).
20. M. Bogey, C. Demuynck and J.L. Destombes, *Mol. Phys.* **43**, 1043 (1981).
21. K. V. L. N. Sastry, E. Herbst and F. C. De Lucia, *J. Chem. Phys.* **75**, 4169 (1981).
22. E. Hirota and Y. Endo, *J. Mol. Spec.* **127**, 527 (1988).
23. T. Amano, *J. Chem. Phys.* **79**, 3595 (1983).
24. S. Gudeman, M. H. Begemann, J. Pfaff and R. J. Saykally, *Phys. Rev. Lett.* **50**, 727 (1983).
25. S. C. Foster, A. R. W. McKellar and T. J. Sears, *J. Chem. Phys.* **81**, 578 (1984).
26. P. B. Davies, P. A. Hamilton and W. J. Rothwell, *J. Chem. Phys.* **81**, 1598 (1984).
27. P. B. Davies and W. J. Rothwell, *J. Chem. Phys.* **81**, 5239 (1984).
28. K. Kawaguchi, C. Yamada, S. Saito and E. Hirota, *J. Chem. Phys.* **82**, 1750 (1985).
29. J. Liu S. T. Lee and T. Oka, *J. Mol. Spec.* **128**, 236 (1988).
30. Puzzarini, R. Tarroni, P. Palmier, S. Carter and L. Dore, *Mol. Phys.* **87**, 879 (1996).
31. J. M. L. Martin, P. R. Taylor and T. J. Lee, *J. Chem. Phys.* **99**, 286 (1993); **99**, 9326 (1993).
32. M. Mladenovic and S. Schmatz, *J. Chem. Phys.* **109**, 4456 (1998).
33. Y. Yamaguchi, C. A. Richards and H. F. Schaefer III, *J. Chem. Phys.* **101**, 8945 (1994).
34. W. P. Watson, *Astrophys. J.* **188**, 35 (1974).
35. S.C. Foster and A.R.W. McKellar, *J. Chem. Phys.* **81**, 3424 (1984).
36. K. Kawaguchi, A.R.W. McKellar and E. Hirota, *J. Chem. Phys.* **84**, 1146 (1986).
37. M. Bogey, C. Demuynck and J.L. Destombes, *Mol. Phys.* **43**, 1043 (1981).
38. K. V. L. N. Sastry, E. Herbst and F. C. De Lucia, *J. Chem. Phys.* **75**, 4169 (1981).
39. E. Hirota and Y. Endo, *J. Mol. Spec.* **127**, 527 (1988); Y. Endo and E. Hirota, *J. Mol. Spec.* **127**, 540 (1988).

40. L. Dore and G. Cazzoli, *Chem. Phys. Lett.* **257**, 460 (1996).
41. J.M. Dyke, N.B.H. Jonathan, A. Morris and M.J. Winter, *Mol. Phys.* **39**, 629 (1980).
42. P. Sebald, 1990, Ph.D. Dissertation, Universität Kaiserslautern.
43. H. Matsui, E. E. Mayer and E. R. Grant, *J. Mol. Spectrosc.* **175**, 203 (1996).
44. W. T. M. Fernando and P. F. Bernath, *J. Mol. Spectrosc.* **145**, 392 (1991).
45. L. Bigio and E. R. Grant, *J. Chem. Phys.* **83**, 5361 (1985); E. R. Grant, in *Advances in Multiphoton Processes and Spectroscopy*, S. H. Lin, ed. (World Scientific, Singapore, 1988).
46. J. Weiss, R. Schinke and V. A. Madelshtam, *J. Chem. Phys.* **113**, 4588-4597 (2000).
47. B. M. Stone, M. Noble and E. K. C. Lee, *Chem. Phys. Lett.* **118**, 83 (1985); H. Rumbles, J. J. Valentini, B. M. Stone and E. K. C. Lee, *J. Phys. Chem.* **93**, 1303 (1989).
48. S. Williams, J. D. Tobiason, J. R. Dunlop, and E. A. Rohlfing, *J. Chem. Phys.* **102**, 8342-8358 (1995); J. D. Tobiason, J. R. Dunlop, and E. A. Rohlfing, *J. Chem. Phys.* **103**, 1448-1469 (1995).
49. D. W. Neyer, X. Luo, I. Burak, and P. L. Houston, *J. Chem. Phys.* **102**, 1645-1657 (1995).
50. R. Vasudev and R. N. Zare, *J. Chem. Phys.* **76**, 5267-5270 (1982).
51. A. M. Schmoltner, P. M. Chu, R. J. Brudzynski and Y. T. Lee, *J. Chem. Phys.* **91**, 6926-6936 (1989).
52. L. F. DiMauro, M. Heaven, and T. A. Miller, *J. Chem. Phys.* **81**, 2339-2346 (1984).
53. D. Forschungsgemeinschaft, and Fonds der Chemischen Industrie, *J. of Molecular Spect.* **209**, 278-279 (2001).
54. R. Wan, X. Chen, F. Wu, B. R. Weiner, *Chem. Phys. Lett.* **260**, 539-544 (1996); K. L. Barnhard, M. He, and B. R. Weiner, *J. Phys. Chem.* **100**, 2784-2790 (1996).
55. D. L. Osborn, H. Choi, D. H. Mordaunt, R. T. Bise, and D. M. Neumark; C. M. Rohlfing, *J. Chem. Phys.* **106**, 3049-3066 (1997).
56. L. R. Brock and E. A. Rohlfing, *J. Chem. Phys.* **106**, 10048-10065 (1997).
57. M. B. Pushkarsky, A. M. Mann, J. S. Yeston, C. B. Moore *J. Chem. Phys.* **115**, 10738 (2001).

58. H. Su, and R. Bersohn, *J. Chem. Phys.* **115**, 217-224 (2001).
59. H. Matsui, J. M. Behm and Edward R. Grant, *Intl. J. Mass. Spec. and Ion Proc.* **159** 37 (1996).
60. E. E. Mayer, H. Hedderich and E. R. Grant, *Phil. Trans. Roy. Soc. A* **355**, 1569 (1977).
61. R. S. Tapper, R. L. Whetten and E. R. Grant, *J. Phys. Chem.* **88**, 1273 (1984).
62. Ionization energies estimated by means of Gaussian 98, Revision A.7 using Density Functional Theory with a B3LYP/6-31G\*\* basis set: P. B. Brint and E. R. Grant, unpublished results.
63. J. W. Hudgens and C. S. Dulcey, *J. Phys. Chem.* **89**, 1505 (1985); A. D. Sappey and J. C. Weisshaar, *J. Phys. Chem.* **91**, 3731 (1987).